

# Microscopic description of rotation: From ground states to the extremes of ultra-high spin

A. V. Afanasjev\*

*Department of Physics and Astronomy, Mississippi State University, MS 39762*

PACS REF: 21.10.Pc, 21.10.Re, 21.60.Jz, 27.90.+b, 27.70.+q

## Abstract

Recent progress in the microscopic description of rotational properties within covariant density functional theory (CDFT) is presented. It is shown that it provides an accurate description of rotational bands both in the paired regime at low spin and in the unpaired regime at ultra-high spins. The predictive power of CDFT is verified by comparing the CDFT predictions for band crossing features in the  $A \geq 242$  actinides with new experimental data. In addition, possible role of the Coulomb antipairing effect for proton pairing is discussed.

## 1. Introduction

Low-energy theoretical nuclear physics aims at the description of different aspects of the nuclear many-body problem for a wide variety of nuclei ranging from the proton to the neutron drip line [1, 2] and beyond. There is also a strong correlation between the advent of new experimental facilities and theoretical developments supporting new physics studied by these facilities at the limits of charge, isospin, spin, deformation etc. The investigation of rotating nuclei is an important avenue for these studies at the limits. For example, rotational properties serve as an important tool for configuration assignments in odd-mass light superheavy nuclei [3, 4]. The stability of nuclei against fission at high spin [5] and the role of proton-neutron pairing [6, 7] can also be addressed by studying rotating nuclei.

So far, the majority of theoretical studies of rotating nuclei have been performed within phenomenological approaches based on the Nilsson or Woods-Saxon potentials. Alternative and more microscopic approaches are based on nonrelativistic [8] and relativistic (covariant) [9] density functional theories (DFT); the latter is usually called covariant DFT (CDFT). Until recently, these approaches were only occasionally used for the description of rotational structures in the pairing regime and no systematic assessment of their errors and the sources of these errors is available. They were mostly applied to superdeformed (SD) rotational bands in different mass regions (see Refs. [4, 9] and references therein), the spins and parities of which are not known in most cases. Prior to Ref. [4], the studies of the normal-deformed (ND) bands in even-even

and especially odd-mass nuclei over the observable frequency ranges have been performed only in a few nuclei (see Ref. [4] for full list of studied nuclei).

The systematic investigation [4] of normal-deformed rotational bands in even-even and odd-mass actinides and light superheavy nuclei within the CDFT framework, performed for the first time in the density functional theory framework, fills significant gaps mentioned above in our knowledge of the performance of microscopic theories. A short overview of these results with the verification of the predictions of Ref. [4] is presented in Sect. 2. The latter is done by comparing the CDFT predictions with new data on rotational bands in Pu, Cm and Cf even-even nuclei. The role of the Coulomb antipairing effect for proton pairing is discussed in Sect. 3. The performance of CDFT in the description of triaxial superdeformed (TSD) rotational bands at ultra-high spin is analyzed in Sect. 4. Finally, the conclusions are presented in Sect. 5.

## 2. Upbendings in actinides: confronting predictions with new experimental data

Fig. 1 shows the results of the first ever (in any DFT framework) systematic investigation of rotational properties of even-even nuclei at normal deformation [4]. The calculations are performed within the cranked relativistic Hartree-Bogoliubov (CRHB) approach with approximate particle number projection by means of the Lipkin-Nogami method (further CRHB+LN) [12]. Cyan dots show new experimental data from Ref. [11] which were not included in Ref. [4]. These data will be analyzed in detail in the current manuscript. One can see that the moments of inertia below band crossings are reproduced well. The upbendings observed in a number of rotational bands of the  $A \geq 242$  nuclei are also reasonably well described in model calculations. However, the calculations also predict similar upbendings in lighter nuclei, but they have not been seen in experiment. The analysis suggests that the stabilization of octupole deformation at high spin, not included in the present CRHB+LN calculations, could be responsible for this discrepancy between theory and experiment [4]. With few exceptions, the rotational properties of one-quasiparticle configurations, which yield important information on their underlying structure and, thus, provide an extra tool for configuration assignment, are also

\*e-mail: [afanasjev@erc.msstate.edu](mailto:afanasjev@erc.msstate.edu)

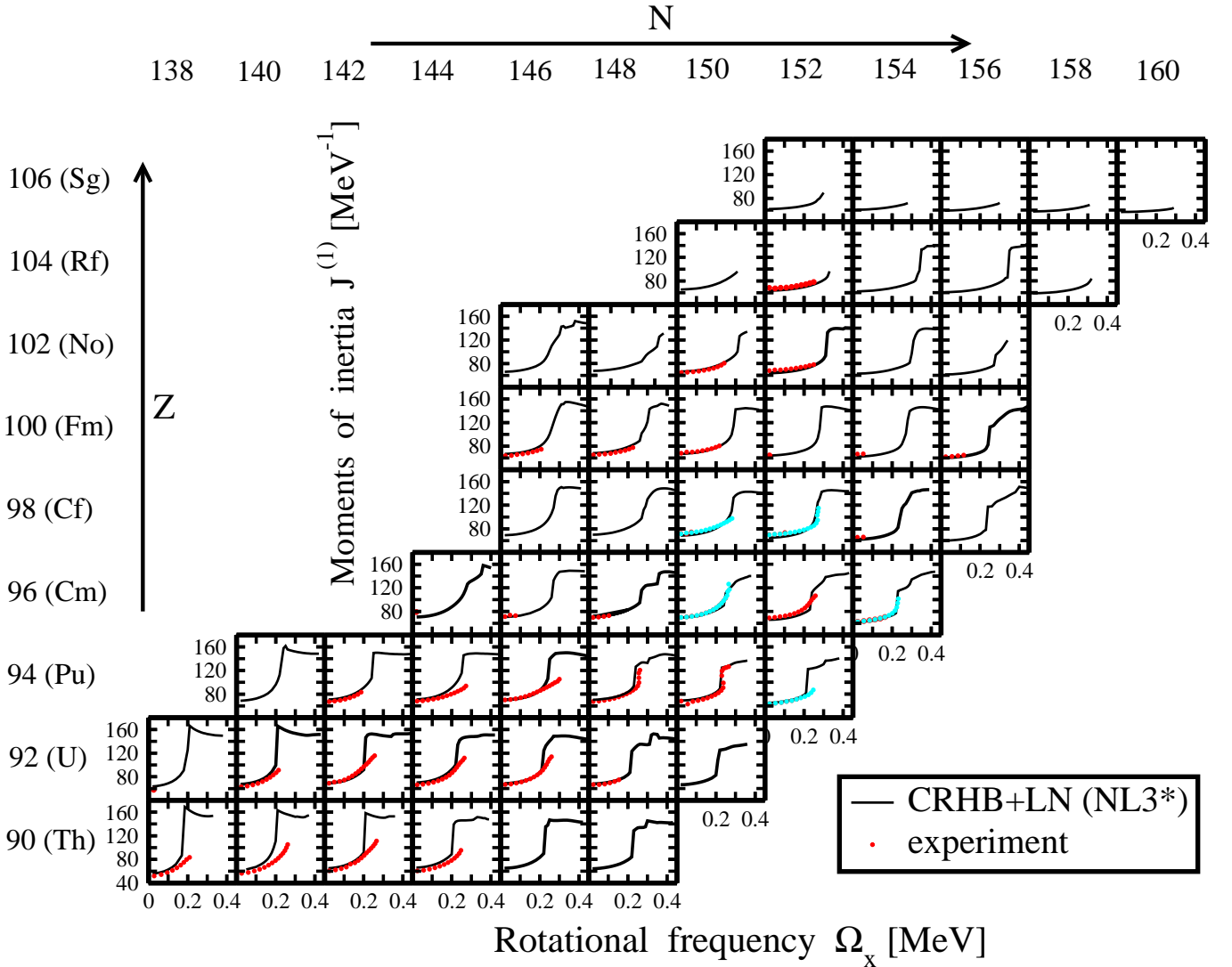


Fig. 1: The experimental and calculated moments of inertia  $J^{(1)}$  as a function of rotational frequency  $\Omega_x$ . The calculations are performed with the NL3\* parametrization [10] of CDFT. Calculated results and experimental data are shown by black lines and red dots, respectively. Cyan dots are used for new data from Ref. [11].

well described in the CRHB+LN calculations (see Ref. [4] for details).

New experimental data on high-spin structures in even-even actinides [11], not analyzed in Ref. [4], include the ground state rotational bands in  $^{246}\text{Pu}$ ,  $^{246,250}\text{Cm}$  and  $^{248,250}\text{Cf}$  (cyan dots in Fig. 1). It should be kept in mind that one or several of the highest spin transition(s) are tentative. It is interesting to compare these data with the predictions of our CRHB+LN calculations [4] and the ones of the cranked shell model with the pairing correlations treated by a particle-number conserving method (further CSM+PNC) [13]. The main difference between these two models is the treatment of the single-particle states. The NL1 [14] and NL3\* [10] parametrizations of the CDFT theory have been fitted only to bulk properties of around ten spherical nuclei [single-particle information such as the energies of single-particle states or spin-orbit splittings has not been used in the CDFT fits]. On the contrary, the pa-

rameters of the Nilsson potential were carefully adjusted to the experimental energies of deformed one-quasiparticle states of actinides in Ref. [13]. Note that the predictions of the CSM+PNC model are available only for the Cm and Cf isotopes. Another major difference between the two models is the treatment of deformation. The deformations are chosen to be close to experimental values and do not change with rotational frequency in the CSM+PNC calculations, while equilibrium deformations are defined fully self-consistently at all calculated rotational frequencies in the CRHB+LN calculations. This procedure reveals considerable changes in quadrupole ( $\beta_2$ ) and triaxial ( $\gamma$ ) deformations at the band crossing in the CRHB+LN calculations (see Fig. 7 in Ref. [15]) which are completely ignored in the CSM+PNC calculations.

Fig. 2 compares CSM+PNC and CRHB+LN results with new experimental data of Ref. [11]. The  $^{242,244}\text{Pu}$  data have already been analyzed in Sect. 4 of Ref. [4], and

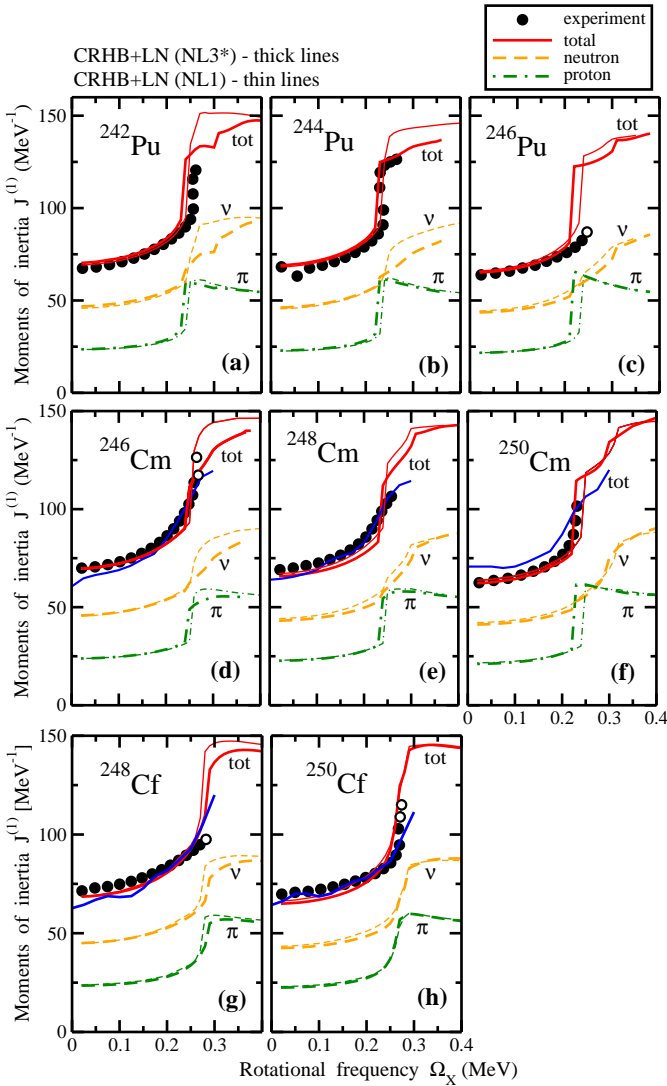


Fig. 2: The experimental and calculated kinematic moments of inertia  $J^{(1)}$  of ground state rotational bands in indicated nuclei as a function of rotational frequency  $\Omega_x$ . Proton and neutron contributions to the kinematic moment of inertia are presented. Open circles are used for tentative experimental points.

are shown in panels (a) and (b) for completeness. The ground state rotational band in  $^{246}\text{Pu}$  has been extended to higher spins in Ref. [11] as compared with earlier data. Its kinematic moment of inertia shows a rapid increase at the highest observed frequencies similar to the one seen before upbendings in  $^{242,244}\text{Pu}$ . However, the  $^{246}\text{Pu}$  data does not reveal an upbend yet. The CRHB+LN calculations predict an upbend in all three even-even Pu isotopes. The upbend in  $^{242,244}\text{Pu}$  is predicted 0.01 – 0.02 MeV earlier in the CRHB+LN(NL3\*) calculations as compared with experiment. A similar situation is expected in  $^{246}\text{Pu}$ . Considering this and the fact that the last observed point in  $^{246}\text{Pu}$  is tentative, one can conclude that there is no significant discrepancies with experimental data. Even better agreement with this new data is seen in the case of the CRHB+LN(NL1) calculations.

A smooth upbending takes place in  $^{248}\text{Cm}$  (Fig. 2e). It is rather well reproduced in the CSM+PNC calculations. The CRHB+LN calculations of Ref. [4] suggest that this upbending is predominantly due to the proton  $i_{13/2}$  alignment. However, the interaction between the  $g$  and  $S$  bands in the band crossing region is too weak in the proton subsystem, which, in contradiction to experiment, leads to a sharp upbending in CRHB+LN calculations. A sharp upbending is also seen in the  $J^{(1)}$  of  $^{250}\text{Cm}$  (Fig. 2f). It is well reproduced in the CRHB+LN calculations. In contrast, the CSM+PNC calculations show a gradual alignment in the band crossing region which contradicts the experiment. The upbending is also present in  $^{246}\text{Cm}$  (Fig. 2d). Both models account for this upbending, but differ in the details of its description. In the CRHB+LN calculations, this upbend is somewhat sharper than in the experiment due to the sharp alignment of the  $i_{13/2}$  proton pair. The CSM+PNC calculations seem to reproduce the gradual character of this alignment better. However, they underestimate the alignment gain at the band crossing. The step in rotational frequency at which the CSM+NPC calculations are performed is not specified in Ref. [13]. If a large step is used, this may be a reason why CSM+NPC calculations look smoother in band crossing region than the CRHB+LN ones. The CRHB+LN calculations are performed in a step of 0.01 MeV in the band crossing region and, as a result, they reveal more details.

The kinematic moment of inertia of the ground state band in  $^{248}\text{Cf}$  (see Fig. 2g) does not reveal an upbend which is predicted both in the CRHB+LN and CSM+PNC calculations. However, considering that the experimental point at the highest frequency is tentative and the difference between calculations and experiment for the point before this one is not too large, a definite conclusion on whether the calculations fail to reproduce the experimental data is not possible. This is especially true considering that the CRHB+LN calculations tend to predict sharp upbends at lower (by 0.01-0.02 MeV) frequency as compared with experiment in this mass region (Fig. 2). The sharp upbend in  $^{250}\text{Cf}$  is well reproduced in the CRHB+LN calculations (see Fig. 2h). On the contrary, the CSM+PNC calculations predict a more gradual increase of  $J^{(1)}$  with frequency which deviates more from experiment relatively to the CRHB+LN calculations.

When comparing CRHB+LN and CSM+PNC calculations, one has to keep in mind that the former provides a much more consistent description of rotational motion in the paired regime. The pairing strength has been fitted to experiment in both approaches [4, 13]. However, the pairing strength is different in even-even and odd-mass nuclei in the CSM+PNC approach [13]; this is a well known deficiency of the cranked shell model (see, for example, Ref. [16]). In contrast, the same pairing strength is used in even-even and odd-mass nuclei in the CRHB+LN approach and, according to Ref. [4], it leads to a consistent and accurate description of odd-even mass staggerings (the  $\Delta^{(3)}$  indicators) and the moments of inertia in even-

even and odd-mass actinides. To our knowledge, this is achieved in a systematic calculations for the first time in the mean field/DFT based models.

A special effort has been made in the CSM+PNC approach to accurately reproduce the energies of deformed one-quasiparticle states. Considering that the strength of the interaction between the  $g$  and  $S$  bands and the crossing frequency depends sensitively on the relative position of aligning high- $j$  orbital with respect to the quasiparticle vacuum [17], one may think that this will improve the description of band crossing properties. However, the comparison of the data with the results of the calculations shows that, on average, the CSM+PNC and CRHB+LN approaches describe observed upbendings with the same level of accuracy (Fig. 2).

In contrast, single-particle information is not used at all in the fits of the CDFT parametrizations [10, 14]. The accuracy of the description of experimental energies of one-quasiparticle deformed states is lower in CDFT as compared with the Nilsson potential (Ref. [18]), which, in particular, is a consequence of the stretching out of the energy scale due to the low effective mass of the nucleon. Despite these facts, the average accuracy of the description of rotational properties in the band crossing region is similar in both models. In addition, an accurate description of the rotational properties in odd-mass nuclei in CRHB+LN [4] is achieved in a more consistent way than in the CSM-NPC model (see discussion above). Whether the alignment in the band crossing region proceeds in a gradual (gradual increase of  $J^{(1)}$ ) or sharp (sharp upbend in  $J^{(1)}$ ) way depends on whether the interaction strength between the  $g$  and  $S$  bands is strong or weak. It follows from the results of both calculations and experiment that this interaction strength shows variations with particle number which are not always reproduced in both model calculations. This is where the differences between the CDFT parametrizations (NL1 and NL3\*) and two models (CRHB+LN and CSM+PNC) with respect to the description of single-particle states show up. For example, they are responsible for the differences in the alignments of the  $j_{15/2}$  neutrons in  $^{242,244}\text{Pu}$  and  $^{246}\text{Cm}$  (Figs. 2a, b and d) which align gradually (sharply) in the CRHB+LN calculations with NL3\* (NL1) parametrization. The high density of the single-particle states in the actinides is another possible factor which decreases the predictive power of the models in the band crossing region.

### 3. Coulomb antipairing effect for proton pairing

The investigation of pairing and rotational properties of actinides in Ref. [4] shows that the strengths of pairing defined by means of the moments of inertia and three-point  $\Delta^{(3)}$  indicators strongly correlate in the CRHB(+LN) framework. This allows to address the role of the Coulomb antipairing effect [19] in the description of pairing in the proton subsystem.

The Coulomb force is not explicitly included into the

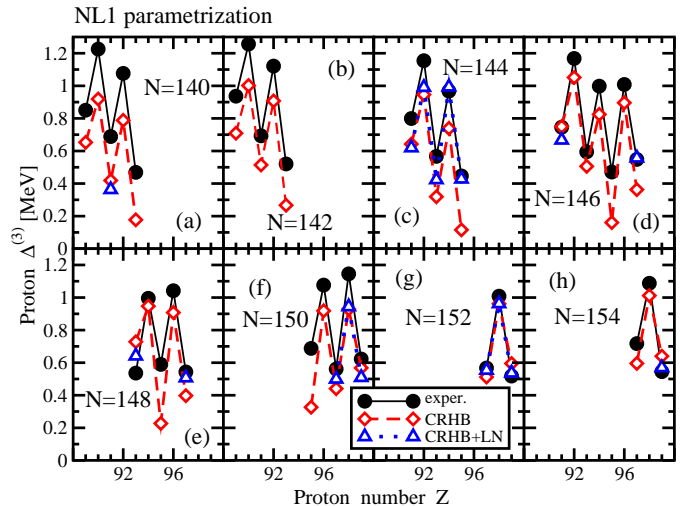


Fig. 3: Experimental and calculated proton three-point indicators  $\Delta_{\nu}^{(3)}(N)$  as a function of neutron number  $N$ . The results of the CRHB and CRHB+LN calculations with the NL1 parametrization are shown. From Ref. [4].

pairing channel of most DFT calculations because of its non-local nature. However, it is known that proton pairing gaps are reduced by 20-30% if an exact Coulomb term is included into the calculations of the pairing field [19, 20, 21]; this term leads to the so-called Coulomb antipairing effect [19]. Proton pairing energies and the moments of inertia of the proton subsystem are also strongly affected by it [19]. However, the Coulomb term is neglected in the calculations of the pairing field in the RHB framework [9]. Thus, it is important to understand to which extent our approach provides a correct description of proton pairing despite the fact that the Coulomb contribution to pairing is neglected. It turns out that the proton  $\Delta_{\pi}^{(3)}$  indicators are correctly described in the CRHB+LN and CRHB calculations (see Fig. 3 in the current manuscript and Figs. 5, 7, and 8 in Ref. [4]). The effect of the Coulomb interaction can be simulated by a renormalization scheme via a reduction factor of  $\gamma_p = 0.9$  [21] for the proton pairing channel. However, the CRHB and CRHB+LN calculations with this renormalization scheme lead to a frequent collapse of the proton pairing and to the proton  $\Delta_{\pi}^{(3)}$  indicators which are too low as compared with experiment. Thus, the Brink-Booker part of the finite range Gogny D1S force, used in the pairing channel of the CRHB(+LN) calculations, has to be treated as an effective pairing force without the Coulomb part, and as such it works rather well in the description of experimental proton pairing. As discussed in Ref. [19], this is a consequence of fitting strategies of the Gogny force parametrizations which effectively neglect the Coulomb term in the pairing channel. Similar to our results, this reference shows that the inclusion of the Coulomb term in the calculations of pairing worsens the good agreement of theoretical results with experimental data, reinforcing the conjecture that the current fits of the Gogny force should be used without Coulomb terms in the pairing channel.

It is also necessary to recognize that the Coulomb anti-pairing effect has not been proven experimentally due to the difficulties of disentangling this phenomenon from other effects in the  $N \neq Z$  systems. However, even-even  $N = Z$  systems provide an excellent laboratory to test this effect, since the similarity of the proton and neutron single-particle spectra (apart from some constant shift in absolute energies by the Coulomb energy) leads to the fact that proton and neutron pairing energies are almost the same for the proton and neutron subsystems in calculations which do not contain a Coulomb term in the pairing channel (as is the case with the CRHB+LN calculations). As a consequence, the alignment (paired band crossing) of proton and neutron pairs in the ground state rotational bands of the  $N = Z$  nuclei takes place at the same rotational frequency in such calculations, which in turn leads to only one bump in the dynamic moment of inertia  $J^{(2)}$  curve. The proton pairing energies would be substantially lower than the neutron ones in the calculations with the Coulomb term in the pairing channel [19]. As a result, the alignment of the proton pair is expected at higher frequency as compared with the neutron one, leading to a double peaked shape for the dynamic moments of inertia. However, as discussed in detail in Ref. [22] (in particular, see Fig. 3 in Ref. [22] and its discussion) the currently available experimental data on ground state rotational bands in even-even  $N = Z$  nuclei shows only one peak in  $J^{(2)}$  originating from a paired band crossing. This does not support the existence of the Coulomb anti-pairing effect. One may argue that the presence of isoscalar neutron-proton pairing could lead to a situation in which these two peaks in  $J^{(2)}$  merge into one which is broader because of the mixing caused by this type of pairing. However, currently there are no strong evidence for the existence of isoscalar  $np$ -pairing, see review in Ref. [7].

#### 4. The extremes of ultra-high spins

While the rotational bands of the actinides are mostly near-prolate, triaxial superdeformed (TSD) bands represent another class of rotational structures built on static triaxial shapes. Of particular interest are the bands recently observed at ultra-high spins in the  $A \sim 154 - 160$  mass region [23]. The TSD bands 1 and 2 in  $^{158}\text{Er}$  were recently studied in Ref. [24] within the cranked relativistic mean field (CRMF) [25] theory, which represents the limit of the CRHB theory for the case of no pairing [9]. Similar to the actinides (Sect. 2), the NL1 and NL3\* parametrizations of the CDFT were employed in this study.

The degree of accuracy of the description of experimental data is illustrated in Fig. 4. The configuration TSD3(a), involving two protons in  $N = 6$  shell and one neutron in  $N = 7$  shell, i.e.  $\pi 6^2\nu 7^1$ , is a possible candidate for the observed band 1 in  $^{158}\text{Er}$ . The experimental dynamic moment of inertia  $J^{(2)}$  is rather well reproduced by assuming this configuration above the band crossing at low frequencies; the level of agreement with experiment

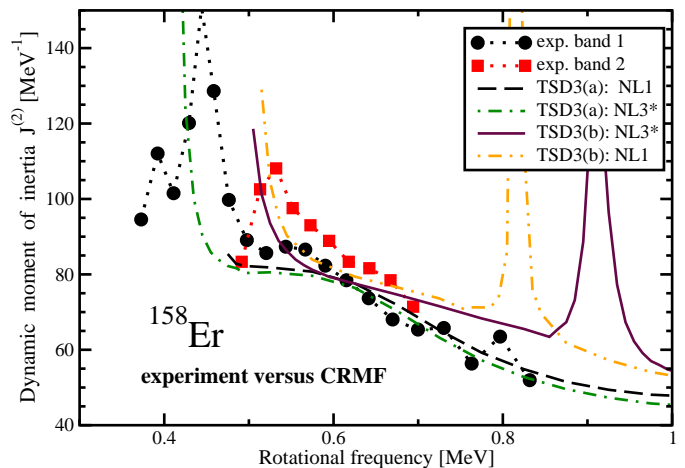


Fig. 4: Experimental dynamic moments of inertia of observed TSD bands in  $^{158}\text{Er}$  (symbols) compared to calculated ones (lines). Based on results presented in Fig. 4 of Ref. [24].

is comparable to that obtained earlier for superdeformed bands in the  $A \sim 150$  region [25, 26]. Our CRMF-NL3\* calculations suggest that the jump in dynamic moment of inertia of band 1 at low frequencies can be associated with a band crossing with large interaction between the  $1/2[770](r = +i)$  and  $[N = 5](r = +i)$  neutron routhians. The calculated transition quadrupole moment  $Q_t$  of TSD3(a) changes from 10.5 eb at  $I = 42$  to 9.0 eb at  $I = 72$  and  $\gamma$  increases slightly from  $12^\circ$  to  $16^\circ$  in this spin range. Considering that the experimental value of  $Q_t \sim 11$  eb [27] is subject to  $\approx 15\%$  uncertainty due to nuclear and electronic stopping powers, these values are reasonably close to experiment. The comparison between experimental and calculated energies shown in Ref. [24] indicates that, to be consistent with TSD3(a), band 1 has to be observed in the spin range  $I = 35 - 77$ . If these theoretical spin assignments turned out to be correct, the experimental TSD band 1 in  $^{158}\text{Er}$  would be the highest spin structure ever observed.

If TSD3(a) is assigned to band 1, then the configuration TSD3(b) built upon TSD3(a) by exciting a neutron from  $N = 5(r = +i)$  into  $5/2[642](r = -i)$  is a natural candidate for experimental band 2. The  $J^{(2)}$  curve of this configuration is close to that of band 2 (Fig. 4), and its transition quadrupole moment is only slightly larger (by  $\sim 0.7$  eb) than that of TSD3(a) which is also close to experiment.

#### 5. Summary

The analysis of rotational spectra within the paired (CRHB+LN) and unpaired (CRMF) cranking versions of the CDFT theory shows that the evolution of the moments of inertia as a function of rotational frequency, particle number and configuration [in odd-mass nuclei] are well reproduced in model calculations both at low and at ultra-high spins. The inaccuracies in the description of the energies of one-quasiparticle states do not substan-

tially affect the calculated moments of inertia outside the band crossing region. Most of the observed upbendings are well reproduced in model calculations. However, in some cases, the details of the alignments (gradual alignment of  $J^{(1)}$  or sharp upbend in  $J^{(1)}$ ) in the band crossing region are not reproduced; this is true for both the CRHB+LN and CSM-NPC approaches. There may be two possible reasons for this observation. First, the interaction strength between the  $g$  and  $S$  bands depends on fine details of the single-particle structure which are not reproduced in model calculations with the required accuracy. Second, because of the limitations of the cranking model in the band crossing region [28], methods beyond mean field may be required for a detailed description of band crossing features in some cases.

The current manuscript illustrates that the cranking model based on CDFT remains a powerful method for the study of rotating nuclei. In our experience, it works well when the mean field is well defined or the configuration interaction is weak; the latter takes place in high-spin structures with negligible pairing. The cranking model does not provide reliable results for nuclei with a very soft potential energy surfaces as exemplified in Ref. [29]. For such nuclei, the beyond mean field methods maybe required [30, 31], as correlations due to configuration mixing and angular-momentum projection can affect the relative energies of the various minima. However, the description of rotational spectra within such models requires the use of a adjustable scaling factor for the moments of inertia, as time-odd mean fields are neglected in the current realizations of these methods [31]. In addition, the calculations of odd-mass nuclei may be problematic in such approaches since they require potential energy surfaces over a substantial deformation space (including also triaxiality) for a fixed blocked one-quasiparticle configuration. However, our experience [4, 18] tells that in medium and heavy mass systems it is frequently impossible to get a convergent solution for such configurations even in local minima; the problem will become even more numerically unstable when constraint(s) on collective coordinate(s) are involved. In addition, the tracing of blocked one-quasiparticle states of a given structure over a large deformation space is highly non-trivial problem in the methods based on the variational principle when triaxiality is involved.

### Acknowledgement

Useful discussions with R. V. F. Janssens and his valuable suggestions for manuscript are gratefully acknowledged. This work has been supported by the U.S. Department of Energy under the grant DE-FG02-07ER41459. This research was also supported by an allocation of advanced computing resources provided by the National Science Foundation. The computations were partially performed on Kraken at the National Institute for Computational Sciences (<http://www.nics.tennessee.edu/>).

### References

- [1] J. Erler *et al*, Nature 486, 509 (2012).
- [2] A. V. Afanasjev, S. E. Agbemava, D. Ray, P. Ring, Phys. Lett. B 726, 680 (2013).
- [3] R. D. Herzberg and P. T. Greenlees, Prog. Part. Nucl. Phys. 61, 674 (2008).
- [4] A. V. Afanasjev and O. Abdurazakov, Phys. Rev. C 88, 014320 (2013).
- [5] J. L. Egido and L. M. Robledo, Phys. Rev. Lett. 85, 1198 (2000).
- [6] S. G. Frauendorf and J. A. Sheikh, Nucl. Phys. A645, 509 (1999).
- [7] A. V. Afanasjev, "Isoscalar and isovector neutron-proton pairing", chapter in "Fifty Years of Nuclear BCS", eds. R. A. Broglia and V. Zelevinsky, in press, see also nuclear theory arkhive arXiv:1205.2134.
- [8] M. Bender, P.-H. Heenen and P.-G. Reinhard, Rev. Mod. Phys. **75**, 121 (2003).
- [9] D. Vretenar, A. V. Afanasjev, G. A. Lalazissis, and P. Ring, Phys. Rep. 409, 101 (2005).
- [10] G. A. Lalazissis *et al* Phys. Lett. **B671**, 36 (2009).
- [11] S. Hota, PhD thesis, University of Massachusetts, Lowell (2012).
- [12] A. V. Afanasjev, P. Ring, and J. König, Nucl. Phys. **A676**, 196 (2000).
- [13] Z.-H. Zhang, X.-T. He, J.-Y. Zeng, E.-G. Zhao, and S.-G. Zhou, Phys. Rev. C 85, 014324 (2012).
- [14] P.-G. Reinhard, M. Rufa, J. Maruhn, W. Greiner and J. Friedrich, Z. Phys. **A323**, 13 (1986).
- [15] A. V. Afanasjev *et al*, Phys. Rev. C 67, 024309 (2003).
- [16] S. K. Tandel *et al*, Phys. Rev. C 82, 041301(R) (2010).
- [17] S. Frauendorf, private communication (2012).
- [18] A. V. Afanasjev and S. Shawaqfeh, Phys. Lett. B 706, 177 (2011).
- [19] M. Anguiano, J. L. Egido, L. M. Robledo, Nucl. Phys. **A683**, 227 (2001).
- [20] T. Lesinski, T. Duguet, K. Bennaceur, and J. Meyer, Eur. Phys. J. **A40**, 121(2009).
- [21] H. Nakada and M. Yamagami, Phys. Rev. **C83**, 031302(R) (2011).
- [22] P. J. Davies *et al*, Phys. Rev. C 75, 011302(R) (2007).
- [23] E. S. Paul *et al*, Phys. Rev. Lett. 98, 012501 (2007).
- [24] A. V. Afanasjev, Yue Shi, and W. Nazarewicz, Phys. Rev. C 86, 031304(R) (2012).
- [25] A. V. Afanasjev, J. König and P. Ring Nucl. Phys. **A608**, 107 (1996).
- [26] A. V. Afanasjev, G. A. Lalazissis, P. Ring, Nucl. Phys. **A634**, 395 (1998).
- [27] X. Wang *et al*, Phys. Lett. B 702, 127 (2011).
- [28] I. Hamamoto, Nucl. Phys. A 271, 15 (1976).
- [29] J. B. Snyder *et al*, Phys. Lett. B723, 61 (2013).

- [30] M. Bender, P. Bonche, P.-H. Heenen, Phys. Rev. C74, 024312 (2006).
- [31] Z. P. Li, T. Niksic, D. Vretenar, J. Meng, G. A. Lalazissis, P. Ring, Phys. Rev. C79, 054301 (2009).